University of Arizona
Tucson, Arizona 85721

IN-35-CR
91251

P.33

FINAL REPORT

Assessment of a Prototype Sunphotometer for Network

Applications - Phase I

Grant Number: NAG 5-1712

Date: August 22, 1991

Prepared by: J.A. Reagan and John Simpson

(NASA-CR-190126) ASSESSMENT OF A PROTOTYPE SUNPHOTOMETER FOR NETWORK APPLICATIONS, PHASE 1 Final Report (Arizona Univ.) 33 p

N92-25610

Unclas

G3/35 0091251

FINAL REPORT ON THE CE SUNPHOTOMETER'S PERFORMANCE AND COMPARISON TO THE U OF A SOLAR RADIOMETER'S DATA

ABSTRACT

Data taken in Tucson, Arizona for comparing the CE sunphotometer's results against the university of Arizona's #3 solar radiometer are in very good agreement. The spectral voltage intercepts ($V_{o\lambda}$) obtained on 15 different days taken with the CE instrument during a seven week period are stable and follow the same daily trends as the $V_{o\lambda}$ for similar wavelengths (λ) contained in the U of A #3 radiometer. The spectral optical depths (τ_λ) obtained from both instruments are also in very good agreement and follow the same trends. The only problem that exists is the CE instrument does not have a heater to stabilize the detector temperature which is important around 1000 nm. Zenith sky radiance scans are in good agreement, but both instruments are biased by direct solar rays entering the instrument's respective entrance aperatures. All diffuse light data shown were, therefore, taken with the instruments shielded from the direct sun. The CE sunphotometer results pertaining to the water vapor λ's are also in good agreement with the U of A #3 and should prove useful for water vapor retrieval.

1. Intercept/Calibration Stability

Table 1 shows the spectral voltage intercepts ($V_{o\lambda}$) obtained for the CE sunphotometer and for similar channel wavelengths (λ) in the University of Arizona #3 solar radiometer for data taken in May through July of 1991 in Tucson, Arizona. The standard Langley technique described in the proposal was used to obtain the intercepts, and they have been normalized to the mean Earth/sun distance. The mean, standard deviation, and the quantity given as standard deviation divided by mean, for these observations are also given in Table 1. The data sets denoted by

the asterik were not included in the statistics as the atmosphere was not sufficiently stable to yield a good, straight-line fit for a Langley plot and, hence, define good intercepts. However, the trends for these days are in good agreement for both instruments.

Figures 1 thru 4 show the $V_{o\lambda}$ changes/trends versus day where day 1 is 5-21-91, day 2 is 5-22-91, etc., for the 4 comparing λ's. The intercepts for the CE instrument have been normalized to the #3 by a factor listed in the figures. It is readily seen from these figures that the intercepts for the comparable λ's from both instruments display similar daily trends caused by aerosol optical depth variations and other effects. In Figure 4, the #3 radiometer has two values given for $V_{o\lambda}$ at 1030.5nm on day 5 and 7. The values denoted by an asterik are the intercepts obtained when the data was corrected for slight detector temperature fluctuations. The #3 instrument has a detector heater for temperature stabilization, but the days were very hot and the radiometer not adequately shaded, so the detector temperature drifted higher by about 2°C. The change in output voltage is $\sim 0.5\%$ per °C and was used to correct the data. The intercepts given in Table 1 are the corrected values.

From Table 1, the quantity standard deviation/mean is seen to be very similar for all λ's for both instruments with a value of $\sim 1\%$, indicating good-stable intercepts. However, the value of 0.015 for 1019.5nm obtained from the CE instrument is higher than the #3 value of 0.011 at the comparable λ. The cause would appear to be that the CE's optical detector is not temperature stabilized. The detector temperature usually varied no more than 2-3°C during afternoon data runs when the atmospheric temperature was stable, as every effort was taken to minimize this effect. However, the CE instrument exhibited a 6-10°C detector temperature rise during the course of the data collection for the two morning data sets shown in Table 1. Since the sunphotometer's output voltage increases with temperature at 1019.5nm by $\sim 0.5\%$ per °C, anomalous $V_{o\lambda}$ and optical depth determinations can be expected when significant temperature changes occur. The $V_{o\lambda}$ obtained on the morning of July 12 were not included in the statistics as the Langley plots were not adequate to yield good intercepts at all λ's. However, if

the intercept obtained on the morning of July 11 is removed from the statistics, the mean $V_{o\lambda}$ changes to 3910mV and the standard deviation drops to 46.1. This yields a value of 0.012 for the quantity standard deviation divided by mean, which is much better than the value obtained with the inclusion of July 11 intercept.

Finally, sample Langley plots yielding the respective $V_{o\lambda}$ values for the four comparison λ's for the CE and #3 instruments are shown in Figures 5 and 6, respectively, for data taken 6-21-91. Good straight-line fits and, hence, good intercepts, were obtained this day; other days as listed in Table 1 typically yielded similar Langley plots.

2. Quality/Accuracy of Optical Depth Retrievals

Figures 7 thru 10 show the trends for optical depth versus day for the CE's 4 non water vapor λ's compared with the similar λ's contained in the #3. Total, Rayleigh only, and total minus Rayleigh τ_λ are given, and it can be seen that they agree very well. The Rayleigh τ_λ varies negligibly, as expected, since the data retrieval site did not change. Hence, both instruments display the same total and aerosol component τ_λ daily changes except for day 14 in Figure 10. In this case, the CE instrument gave a notably higher aerosol and thus total τ_λ than the #3. These data were taken on the morning of July 12 when the detector temperature rose 10°C during the course of the data run, contributing to anomalous $V_{o\lambda}$ and τ_λ retrievals at 1019.5 nm. It should be noted that the optical depths in general are not very accurate due to temporal variations (asterik values in Table 1) for that day. However, the better agreement in the optical depths for λ's other than 1019.5 nm indicate that the 1019.5 nm data for the CE instrument were temperature biased.

In general, the CE sunphotometer shows a slightly higher τ_λ at all the comparing λ's, but this is expected as it's comparing λ's are slightly shorter than the #3's. The asterik values in Figure 10 denotes the temperature corrected data for day 5 for the #3. The day 7 correction was not plotted as it was small enough that it did not vary much from the uncorrected value.

3. Temperature Sensitivity

Figure 10a shows output voltages obtained at various λ's for the CE instrument that were recorded around noon on 7-18-91. The detector temperature was allowed to increase from 17 to 40°C, due to natural heating by exposure to solar radiation, and the V_λ increase at 1019.5 nm is readily seen. The general decrease in V_λ at the other λ's was attributed to a small increase in aerosols as the atmospheric airmass did not change substantially in the 45 minutes it took for the detector temperature to warm to 40°C. Thus, temperature changes do not appear to be affecting the other λ's contained in the CE instrument, as expected for a silicon optical detector. The increase in V_λ at 1019.5 nm was estimated to be about 0.3% per °C, which is typical for a silicon detector at this λ. If a filter around 1000 nm is to be included in the instrument, a detector heater to stabilize the detector temperature would improve the accuracy of the data.

4. General Ease of Operation

The CE Sunphotometer is very easy to use. The speed at which the filters rotate and data collection is performed make it an ideal instrument. The portability of it is also a great advantage. One suggestion is to make the tripod threaded mount hole a bit deeper to insure a more secure fasten to a tripod. A quadrant detector to initiate automatic data collection when solar allignment is achieved would also eliminate manual pointing errors.

5. Zenith Diffuse Light Measurements

Figures 11 thru 18 show spectral zenith diffuse light voltage readings plotted as a function of solar zenith angle for data taken on June 20 and 21, 1991. The data on 6-20-91 were taken at large solar zenith angles and the data taken 6-21-91 were at moderate solar zenith angles. The CE's output voltages were normalized to the #3's by the factors listed in the figures. As with the Langley plot measurements, the data are in good agreement showing similar trends for the comparing λ's. When skylight is completly blocked from entering the instrument's respective entrance

aperatures, the voltage readings read 0 at all λ's for both instruments, indicating no substantial noise or light leakage. From these results, there appears to indeed be a linear relationship between entering solar or diffuse radiation to detector output voltage. However, direct solar rays do bias the measurements for both instruments. Thus, the data shown were collected with the direct sun shielded. Some type of shading device should be added to the CE instrument if it is to be used for diffuse light measurements.

6. Water Vapor Filter Modified/Langley Plot Results

Table 2 displays the voltage ratio intercepts (water vapor over aerosol) obtained for the various dates listed using the modified Langley plot technique (plotting a voltage ratio versus square root of airmass). The voltage ratio intercepts for the CE narrow/CE broad bands are also given in the table. The CE narrow, broad, and narrow/broad band values were multiplied by 1.24, 2.48, and 0.83, respectively, to normalize them to the #3. Figure 19 shows these data plotted versus day, and it is easily seen that the CE narrow and #3 trends are very similar, which is expected as the #3 water vapor filter is narrow. The CE narrow/broad band also follows a somewhat similar trend. If filter profiles can be obtained for the CE sunphotometer, actual precipitable water amounts can be compared with the #3 and radiosonde data. Data is especially desired for the CE narrow/broad band ratio technique as no Rayleigh and aerosol τ_λ differences exist between the two λ's used in the ratio. However, the results obtained by the modified Langley plots indicate that accurate water vapor retrievals can be obtained from the CE suphotometer. Example modified Langley plots are shown for the #3, CE narrow, CE broad, and CE narrow/broad bands in Figures 20, 21, 22, and 23, respectively, for data taken 6-21-91.

7. Conclusions

The various data taken with the CE sunphotometer and #3 solar radiometer are in very good agreement and indicate that the CE sunphotometer should prove useful for the research outlined in the proposal. The portability and ease of use

make it an ideal instrument. If a 1000 nm filter is to be used, a detector temperature stabilizer or some means for correcting the data for detector temperature changes will improve the accuracy of the data. Also, a shield of some sort should be added to block the direct sun if diffuse light measurements are to be made with the instrument.

Table 1

Zero-Airmass Voltage Intercepts (millivolts)

CE Sunphotometer

Day	Date(1991)	439.0	660.5	870.2	1019.5
			wavelength(nm)		
01	5-21*	4104.56	5651.57	3911.81	3690.89
02	5-22	4411.09	5972.58	4092.28	3871.54
03	5-24	4311.32	5896.99	4026.76	3810.09
04	5-29	4436.09	6123.64	4184.65	3948.43
05	6-06	4440.04	6070.16	4141.33	3947.39
06	6-07	4419.07	5999.89	4104.63	3906.56
07	6-17	4438.84	5989.81	4100.86	3968.81
08	6-19	4339.39	5953.55	4080.93	3925.41
09	6-20*	4885.89	6270.39	4177.46	3955.13
10	6-21	4413.33	5989.88	4101.62	3890.01
11	7-02	4496.37	6009.39	4064.05	3888.02
12	7-03	4424.40	6038.12	4094.95	3957.37
13	7-10	4427.08	5994.56	4098.27	3900.49
--	7-11a	4396.60	5991.14	4122.05	3785.07
14	7-12a*	4240.99	5866.09	4018.18	3804.25
15	7-12*	4095.18	5743.33	3970.35	3796.76
	mean	4413	6002	4101	3900
	std dev.	47.9	56.8	38.7	56.9
	std dev/mean	.011	.009	.009	.015

#3 U of A Solar Radiometer

Day	Date(1991)	441.5	671.2	873.0	1030.5
			wavelength(nm)		
01	5-21*	481.28	1327.34	879.88	468.17
02	5-22	522.71	1411.69	923.61	493.57
03	5-24	510.89	1382.06	910.14	487.74
04	5-29	527.56	1443.49	941.21	505.67
05	6-06	524.41	1415.99	930.32	505.78
06	6-07	524.36	1427.88	929.16	498.37
07	6-17	530.54	1423.47	927.86	504.47
08	6-19	520.94	1419.79	921.32	498.82
09	6-20*	575.40	1464.65	945.57	507.05
10	6-21	522.11	1409.97	919.89	496.36
11	7-02	531.56	1399.31	911.67	498.97
12	7-03	520.28	1416.42	913.17	497.42
13	7-10	523.82	1407.32	909.83	493.15
--	7-11a	******	no data taken	with #3	********
14	7-12a*	501.13	1376.97	884.01	487.75
15	7-12*	486.44	1364.87	888.39	485.20
	mean	524	1414	922	498
	std dev.	5.6	15.8	10.0	5.6
	std dev/mean	.011	.011	.011	.011

*--data not included in statistics as these intercepts were bad
a--data taken in morning

Table 2

H2O VOLTAGE RATIO INTERCEPTS

Day	DATE (1991)	#3	CE Narrow	*1.24	CE Broad	*2.48	CE Narrow/ CE Broad	*0.83
02	5-22	1.666	1.348	1.671	0.672	1.667	2.005	1.664
03	5-24	1.503	1.233	1.528	0.642	1.592	1.914	1.589
04	5-29	1.394	1.122	1.391	0.662	1.642	1.696	1.408
05	6-06	1.700	1.367	1.694	0.691	1.714	1.979	1.643
06	6-07	1.674	1.341	1.662	0.701	1.738	1.912	1.587
07	6-17	1.807	1.459	1.808	0.672	1.667	2.157	1.790
08	6-19	1.352	1.104	1.368	0.648	1.607	1.704	1.414
09	6-20	1.667	1.349	1.672	0.703	1.743	1.918	1.592
10	6-21	1.673	1.354	1.678	0.697	1.729	1.941	1.611
11	7-02	1.613	1.341	1.663	0.624	1.548	2.149	1.784
12	7-03	1.593	1.329	1.648	0.596	1.478	2.229	1.850
13	7-10	1.894	1.551	1.923	0.653	1.619	2.375	1.972
--	7-11a	-----	1.592	1.974	0.642	1.592	2.479	2.058
14	7-12a	2.087	1.670	2.071	0.627	1.556	2.663	2.210
15	7-12	1.222	1.013	1.256	0.560	1.390	1.808	1.501

a data taken in morning
--- no data taken with #3 on 7-11-91

Figure 1

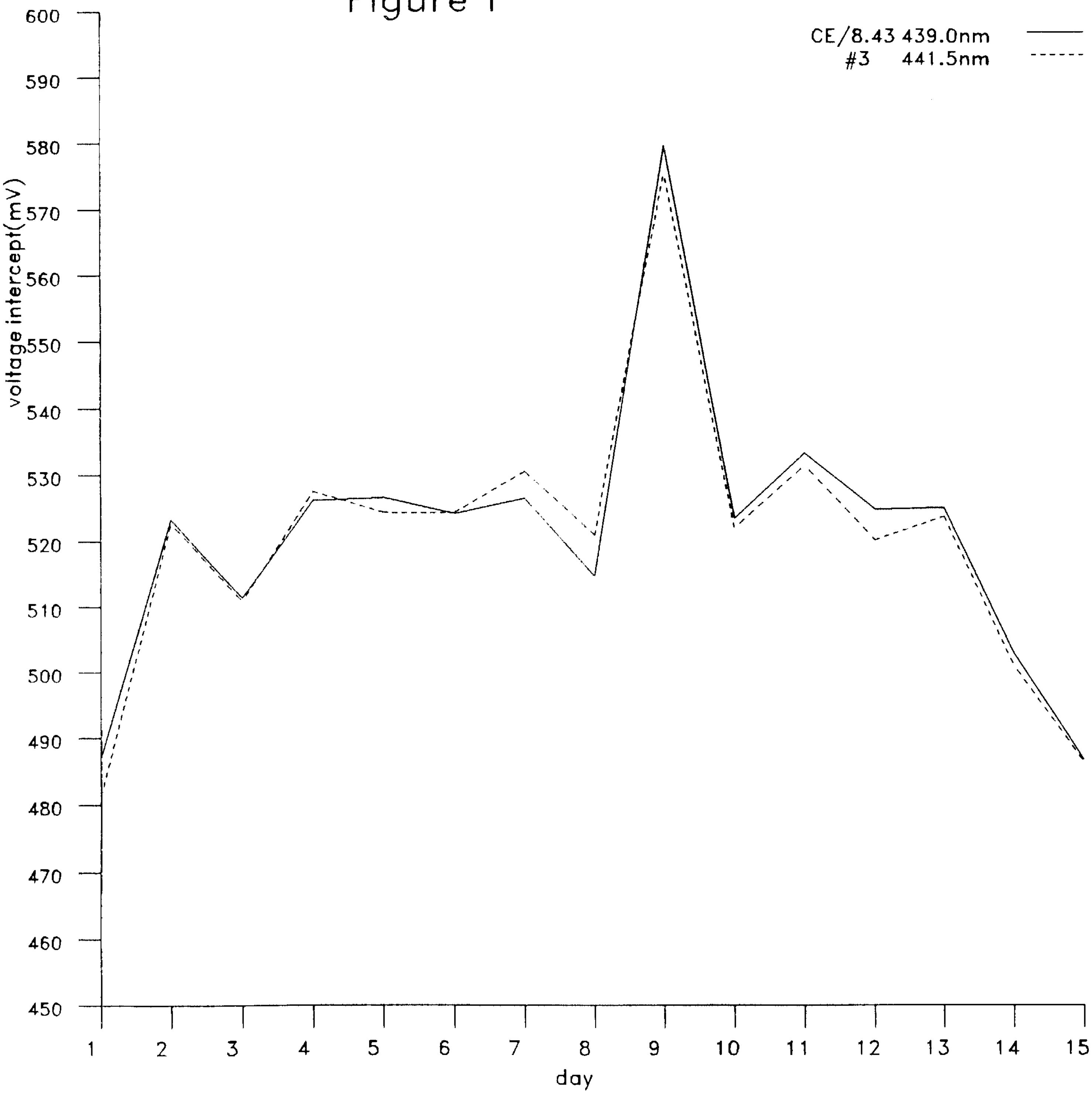

CE/8.43 439.0nm
#3 441.5nm
voltage intercept(mV)
600
590
580
570
560
550
540
530
520
510
500
490
480
470
460
450
1 2 3 4 5 6 7 8 9 10 11 12 13 14 15
day

Figure 2

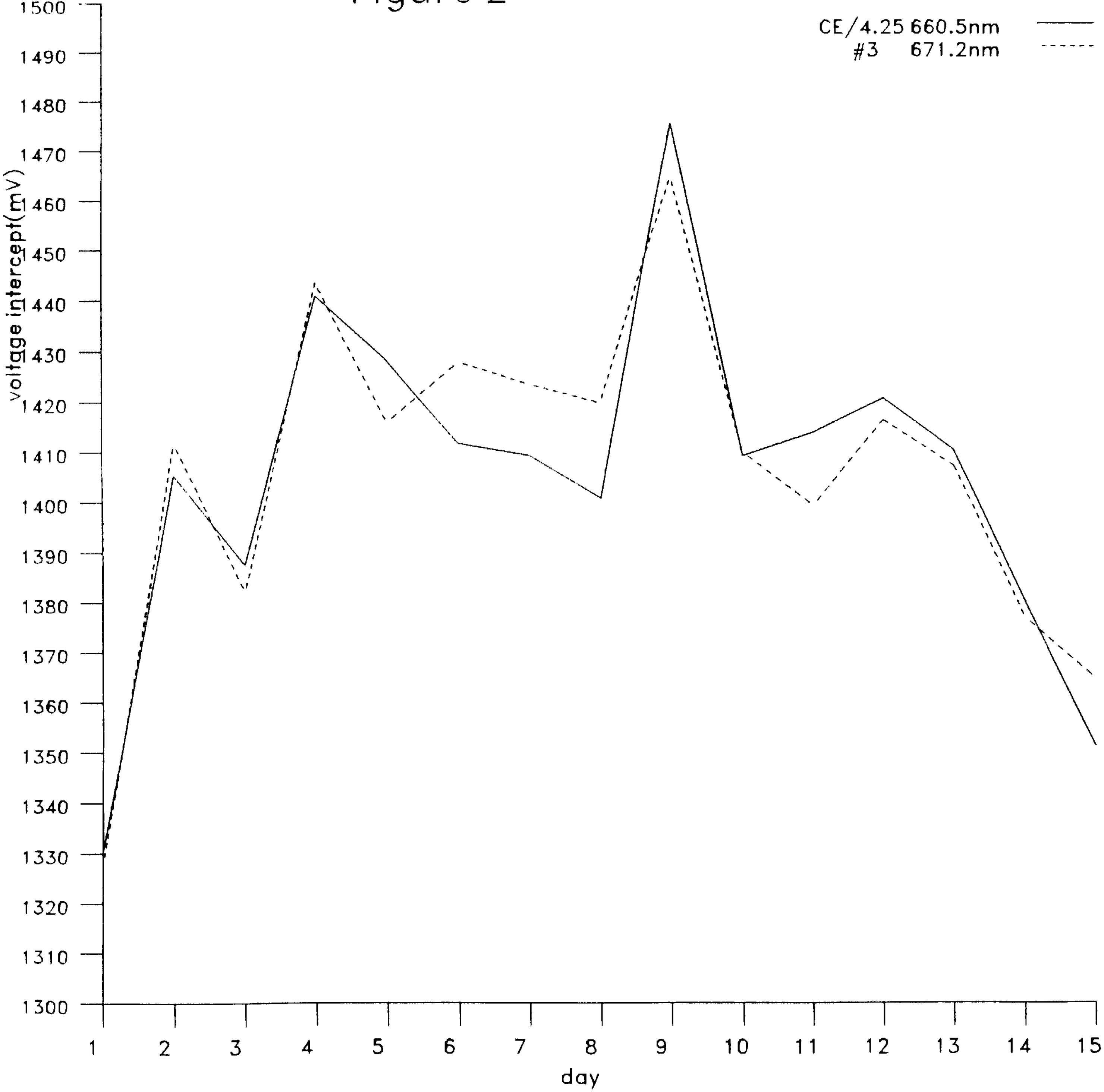

CE/4.25 660.5nm
#3 671.2nm
voltage intercept(mV)
1500
1490
1480
1470
1460
1450
1440
1430
1420
1410
1400
1390
1380
1370
1360
1350
1340
1330
1320
1310
1300
1
2
3
4
5
6
7
8
9
10
11
12
13
14
15
day

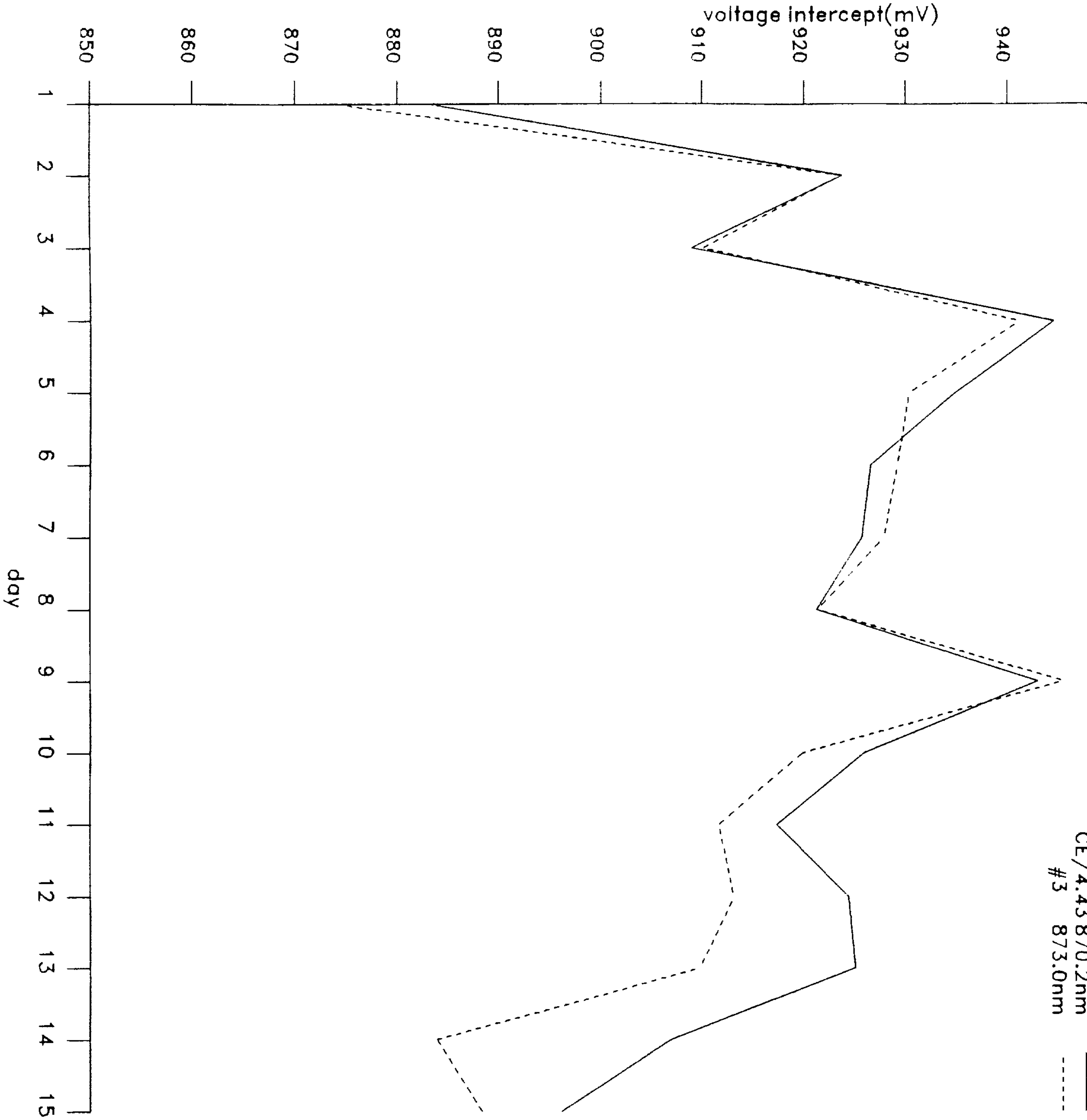

voltage intercept(mV)
950
940
930
920
910
900
890
880
870
860
850
1
2
3
4
5
6
7
8
9
10
11
12
13
14
15
day
CE/4.43 870.2nm
#3 873.0nm

Figure 5

Figure 4

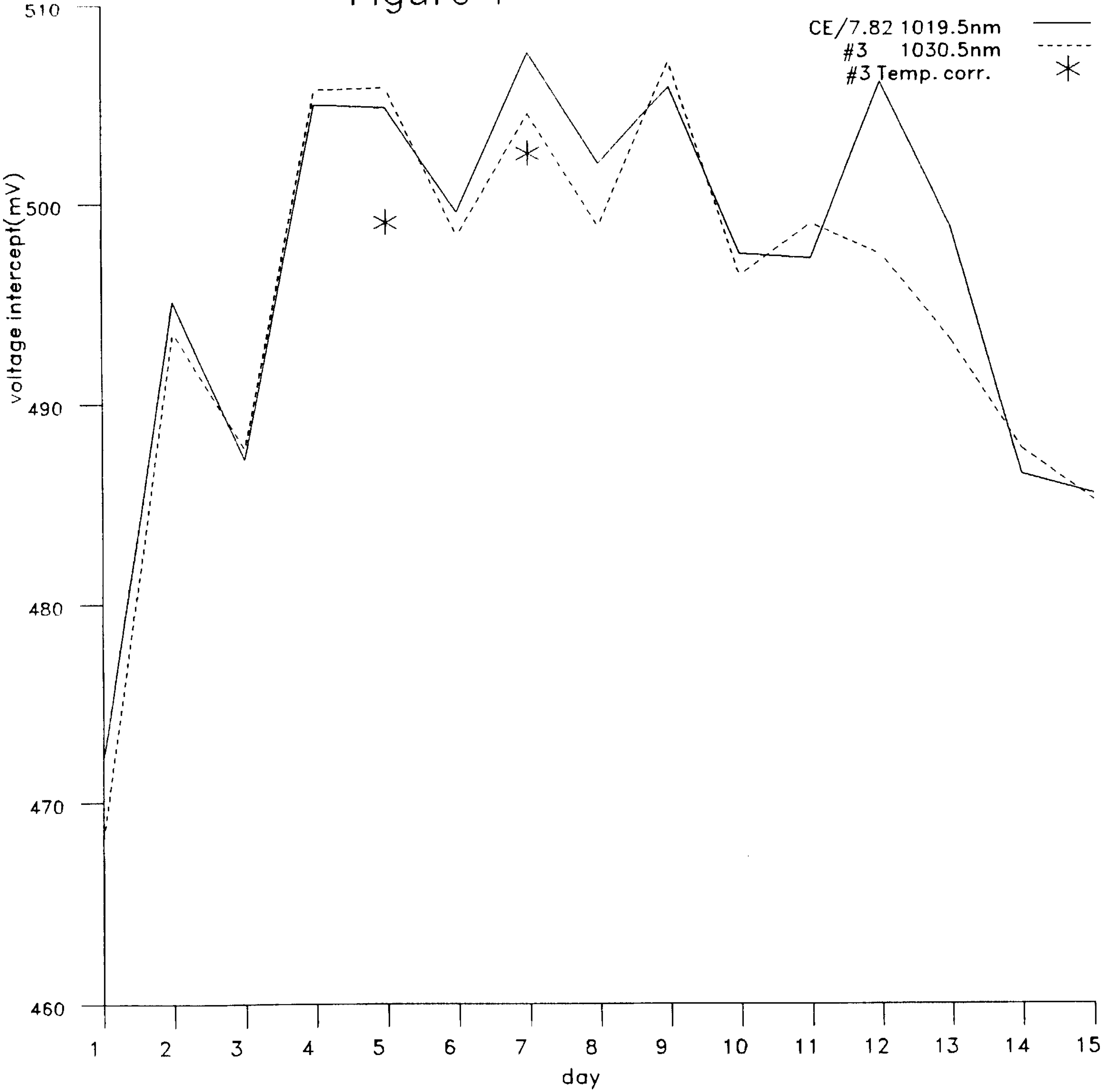

CE/7.82 1019.5nm
#3 1030.5nm
#3 Temp. corr.
voltage intercept(mV)
510
500
490
480
470
460
1
2
3
4
5
6
7
8
9
10
11
12
13
14
15
day

Figure 5   6/21/91   CE

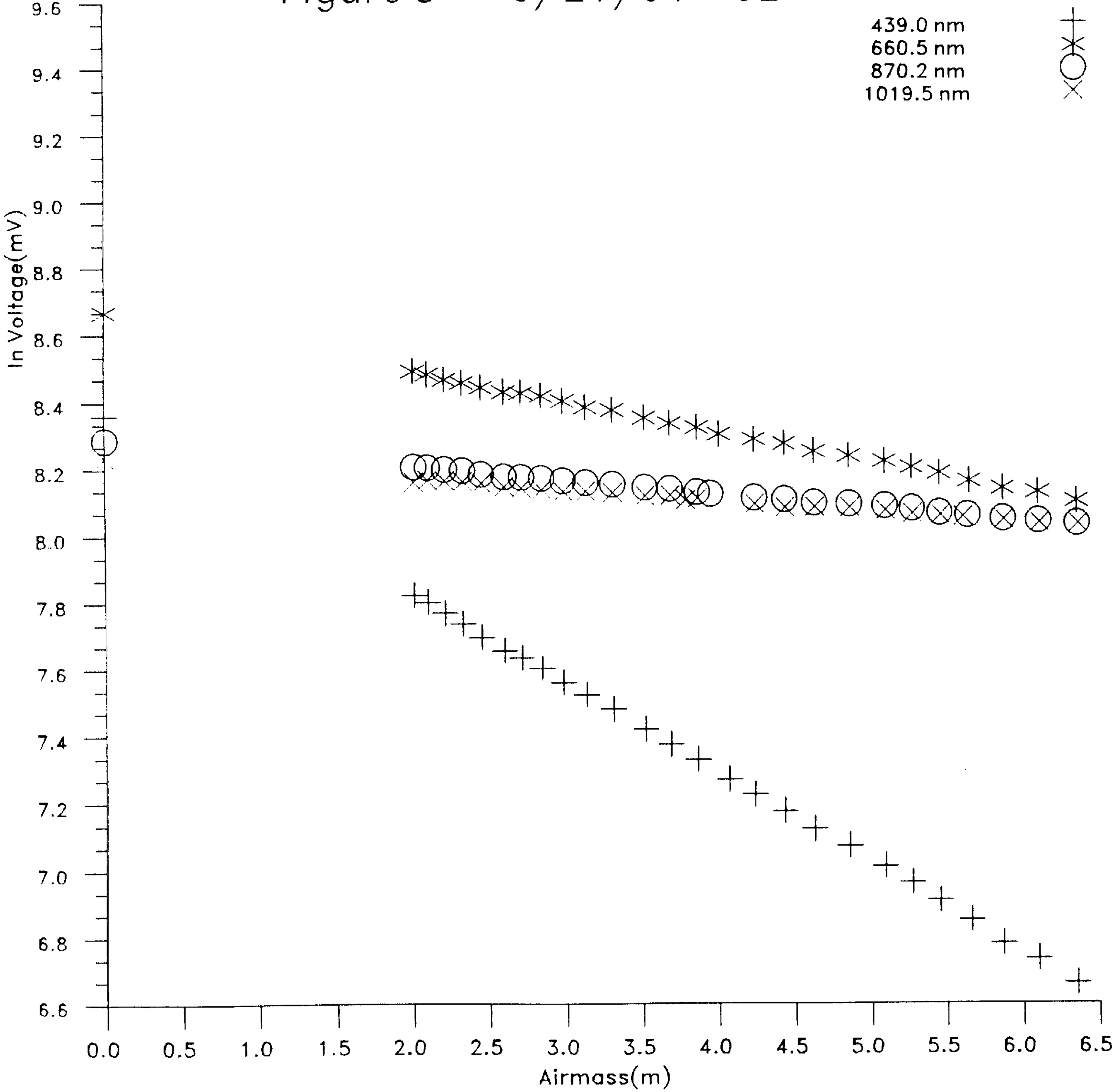

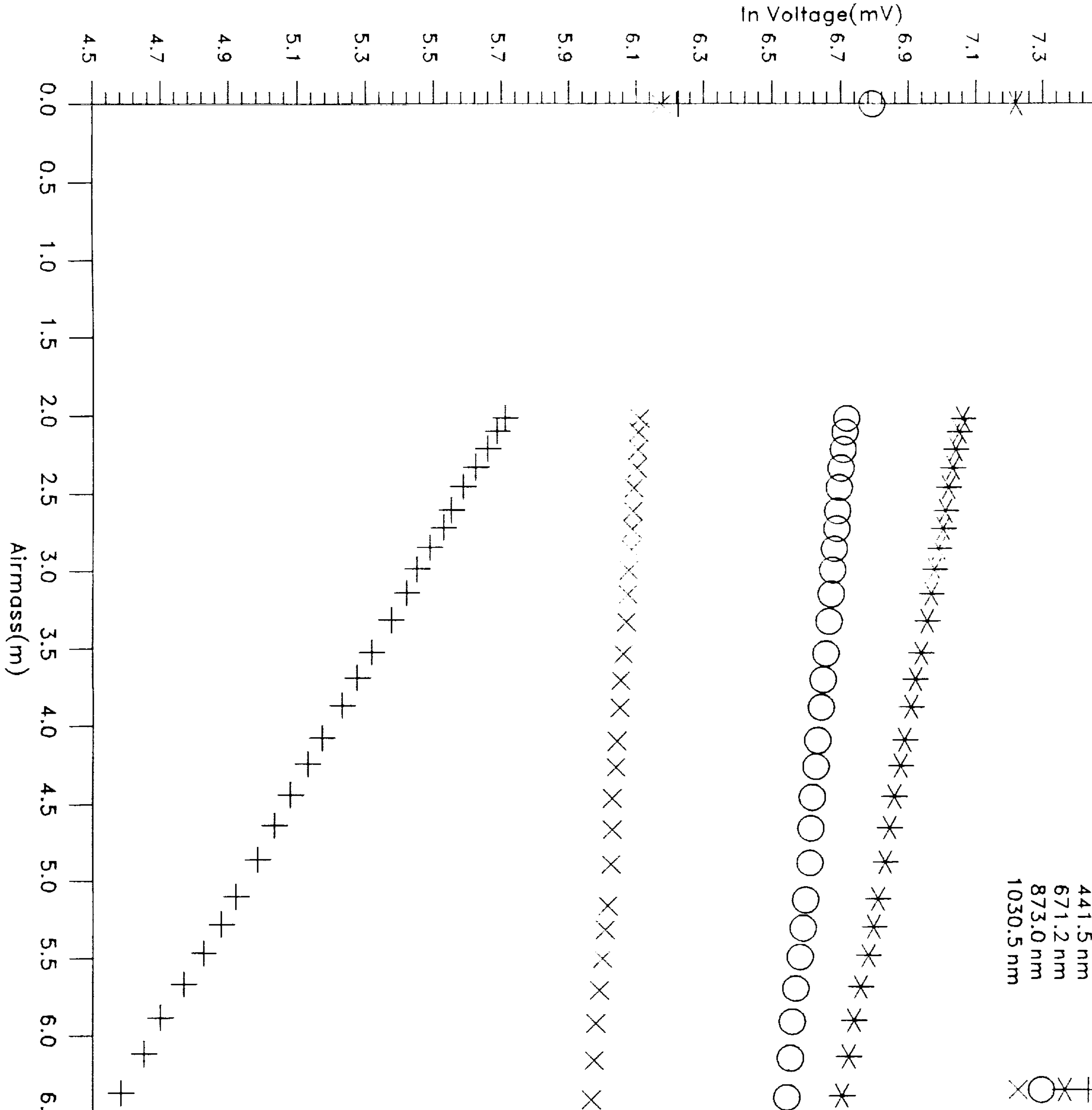

Figure 6 6/21/91 #3

Figure 7

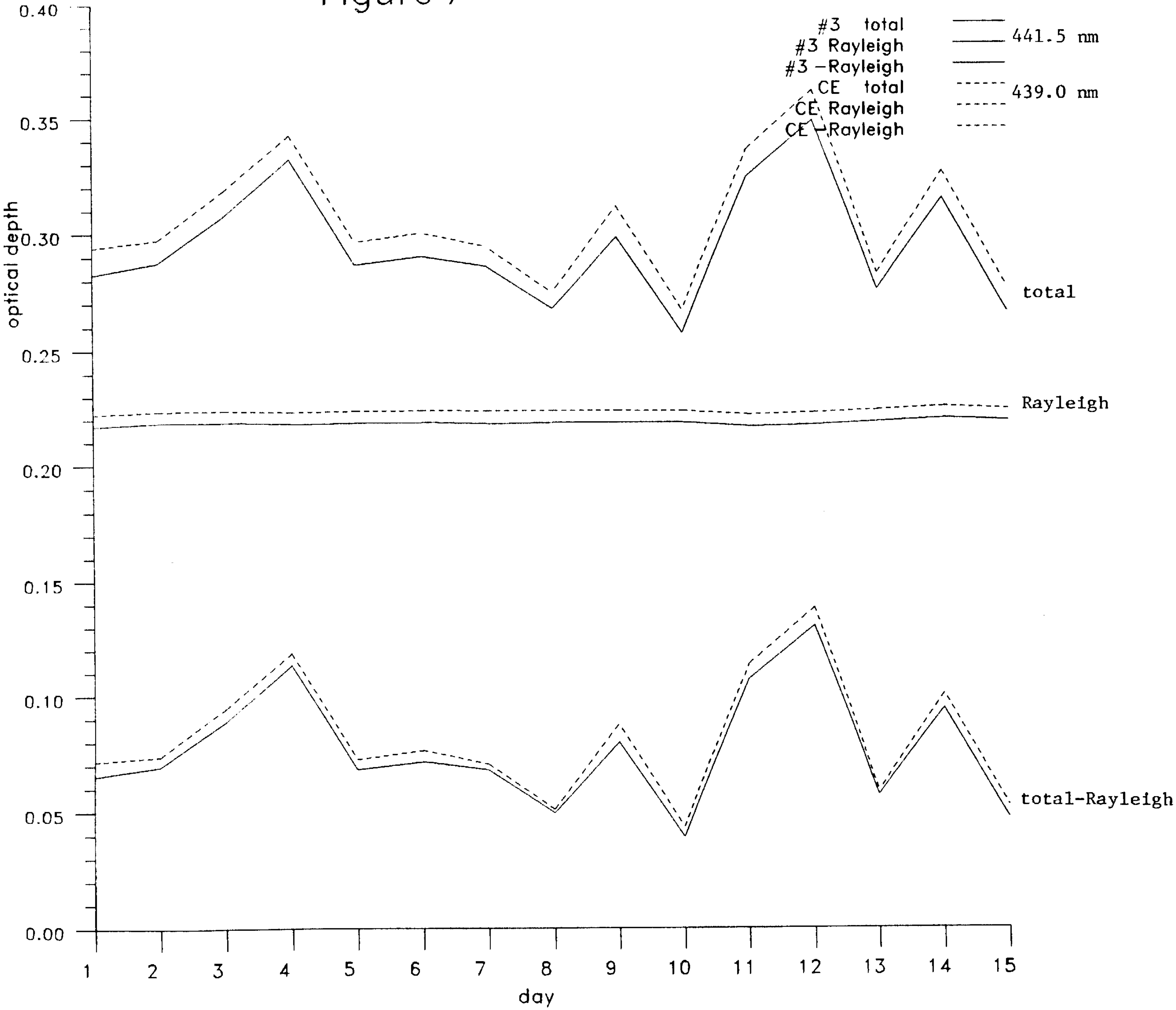

optical depth
0.00
0.05
0.10
0.15
0.20
0.25
0.30
0.35
0.40
day
1
2
3
4
5
6
7
8
9
10
11
12
13
14
15
#3 total
#3 Rayleigh
#3 -Rayleigh
441.5 nm
CE total
CE Rayleigh
CE -Rayleigh
439.0 nm
total
Rayleigh
total-Rayleigh

Figure 8

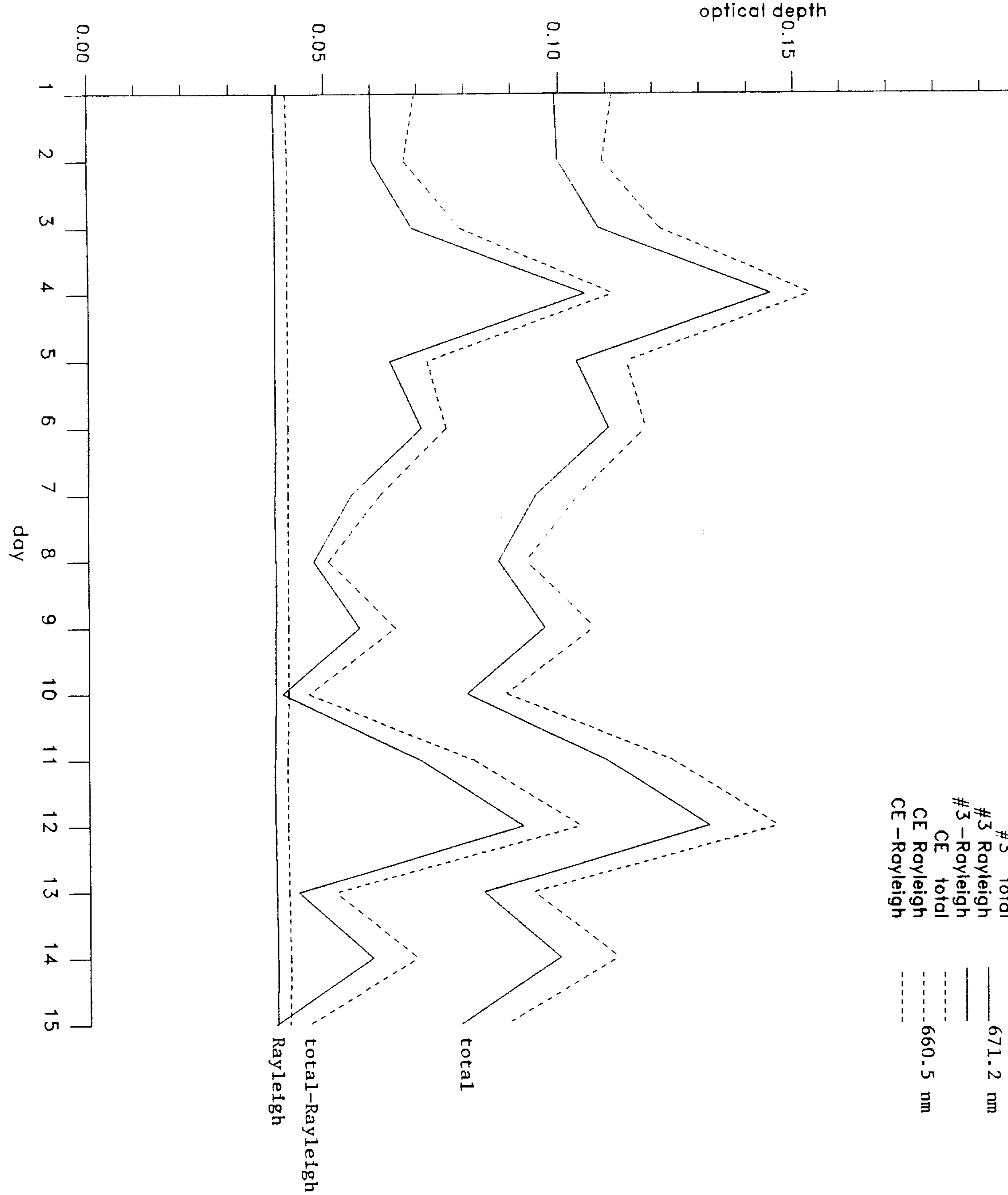
optical depth
0.00
0.05
0.10
0.15
0.20
day
1
2
3
4
5
6
7
8
9
10
11
12
13
14
15
#3 total
#3 Rayleigh
#3 -Rayleigh
CE total
CE Rayleigh
CE -Rayleigh
671.2 nm
660.5 nm
total
total-Rayleigh
Rayleigh

Figure 9

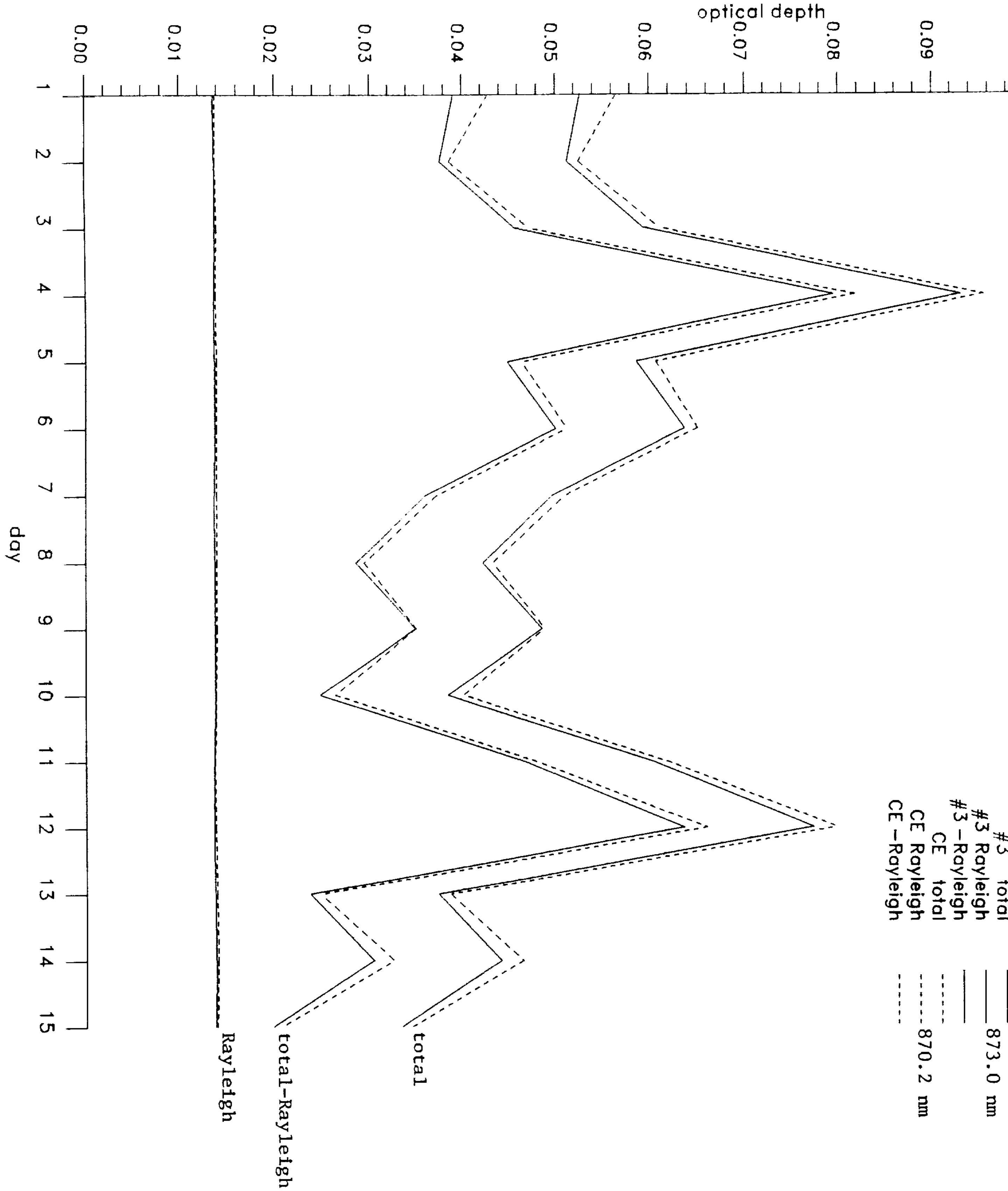
optical depth
0.00
0.01
0.02
0.03
0.04
0.05
0.06
0.07
0.08
0.09
0.10
day
1
2
3
4
5
6
7
8
9
10
11
12
13
14
15
#3 total
#3 Rayleigh
#3 -Rayleigh
CE total
CE Rayleigh
CE -Rayleigh
873.0 nm
870.2 nm
total
total-Rayleigh
Rayleigh

Figure 10

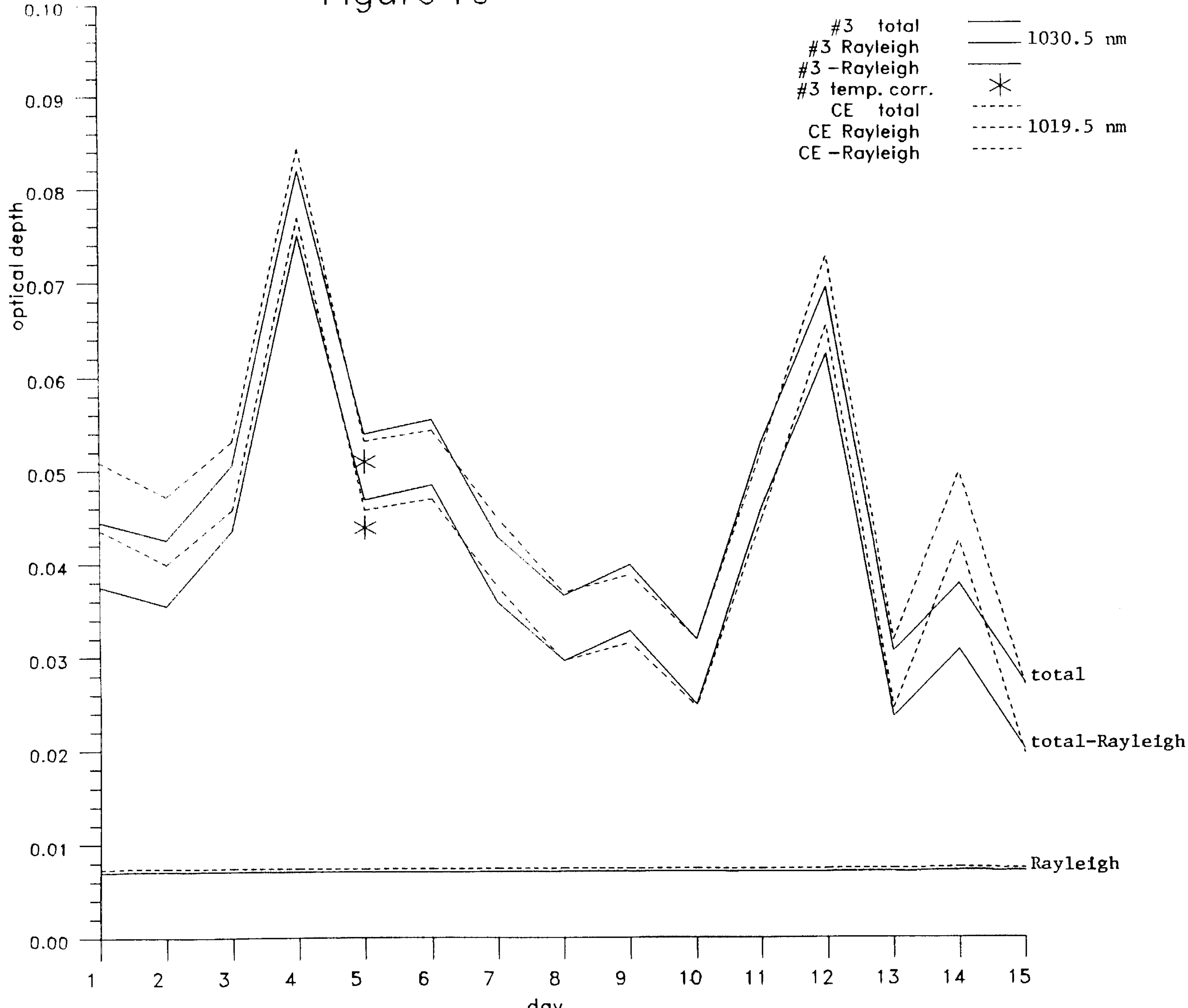

#3 total
#3 Rayleigh
#3 -Rayleigh
#3 temp. corr.
CE total
CE Rayleigh
CE -Rayleigh
1030.5 nm
1019.5 nm
optical depth
0.00
0.01
0.02
0.03
0.04
0.05
0.06
0.07
0.08
0.09
0.10
day
1
2
3
4
5
6
7
8
9
10
11
12
13
14
15
total
total-Rayleigh
Rayleigh

Figure 10a

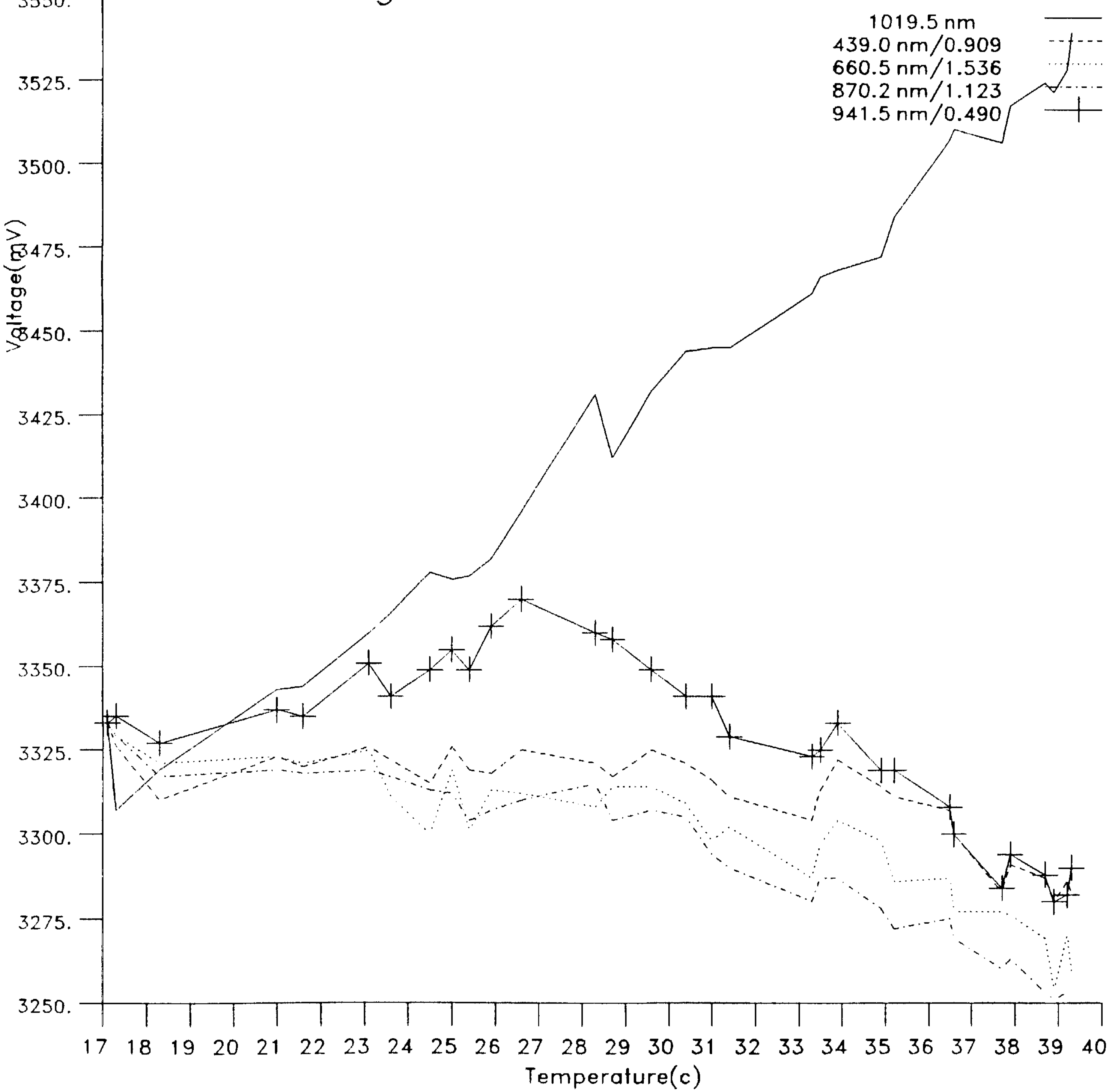
1019.5 nm
439.0 nm/0.909
660.5 nm/1.536
870.2 nm/1.123
941.5 nm/0.490
Voltage(mV)
3550.
3525.
3500.
3475.
3450.
3425.
3400.
3375.
3350.
3325.
3300.
3275.
3250.
17 18 19 20 21 22 23 24 25 26 27 28 29 30 31 32 33 34 35 36 37 38 39 40
Temperature(c)

Figure 11

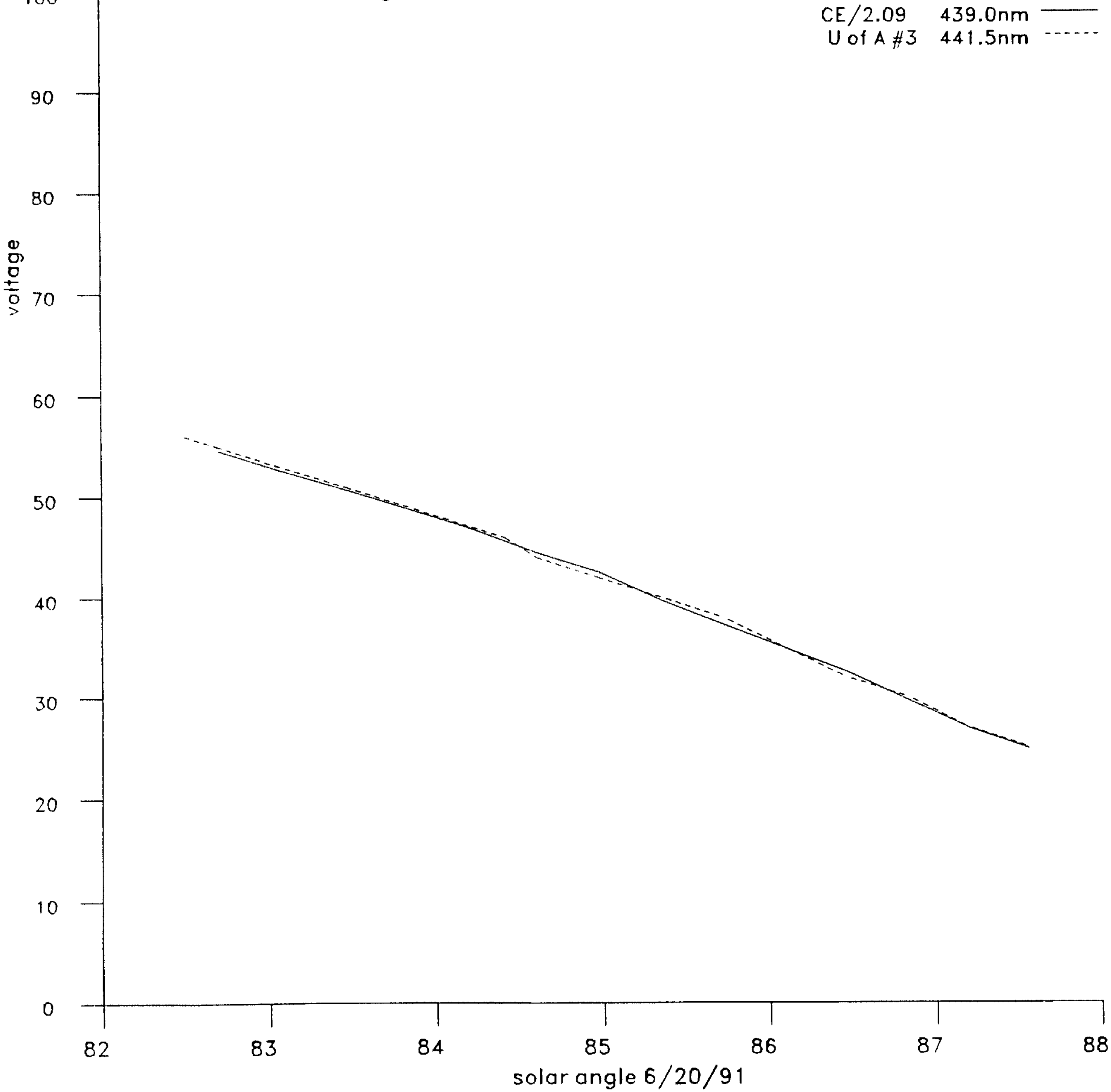
CE/2.09 439.0nm
U of A #3 441.5nm
voltage
100
90
80
70
60
50
40
30
20
10
0
82
83
84
85
86
87
88
solar angle 6/20/91

Figure 12

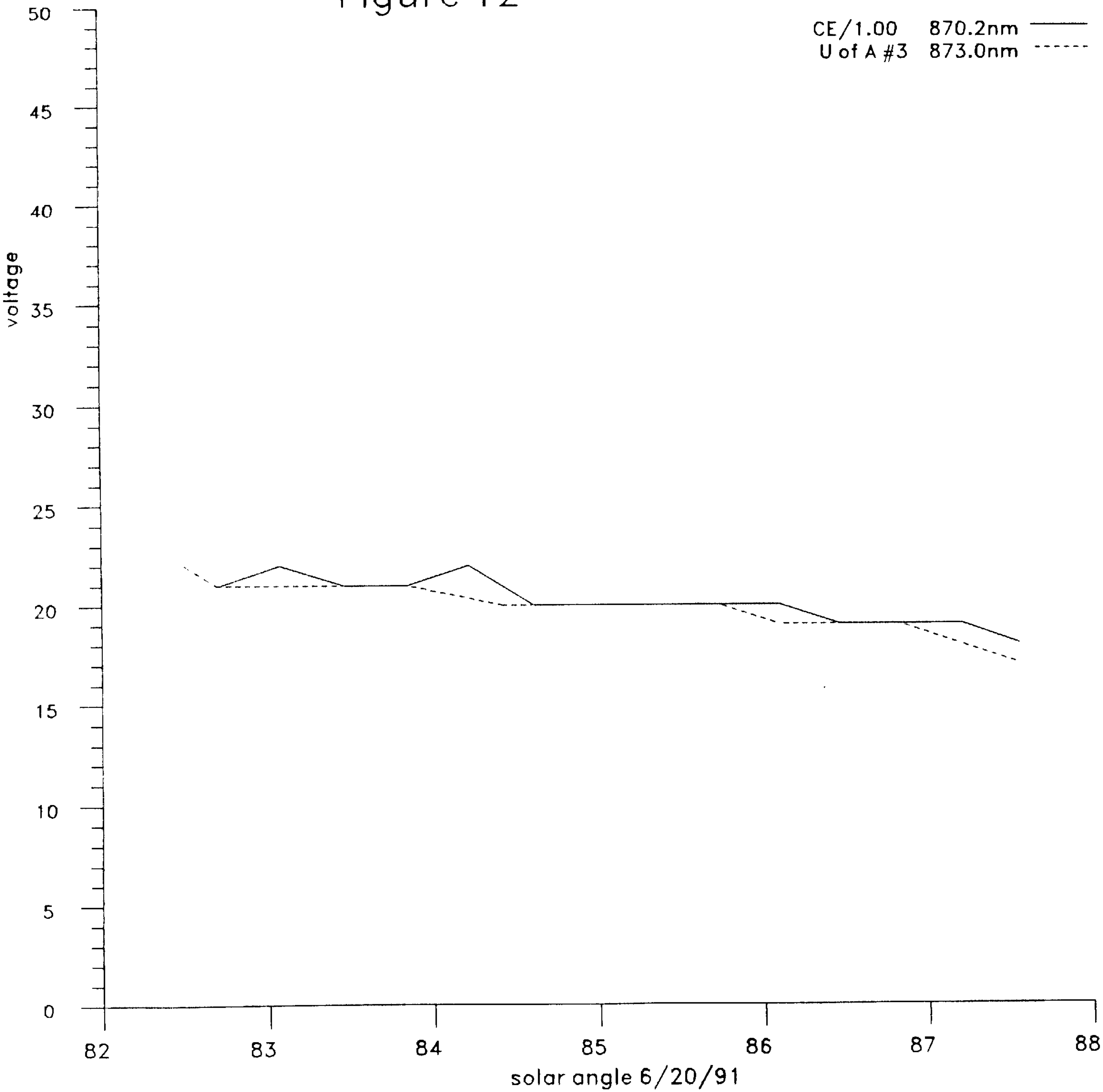

CE/1.00 870.2nm
U of A #3 873.0nm
voltage
0
5
10
15
20
25
30
35
40
45
50
82
83
84
85
86
87
88
solar angle 6/20/91

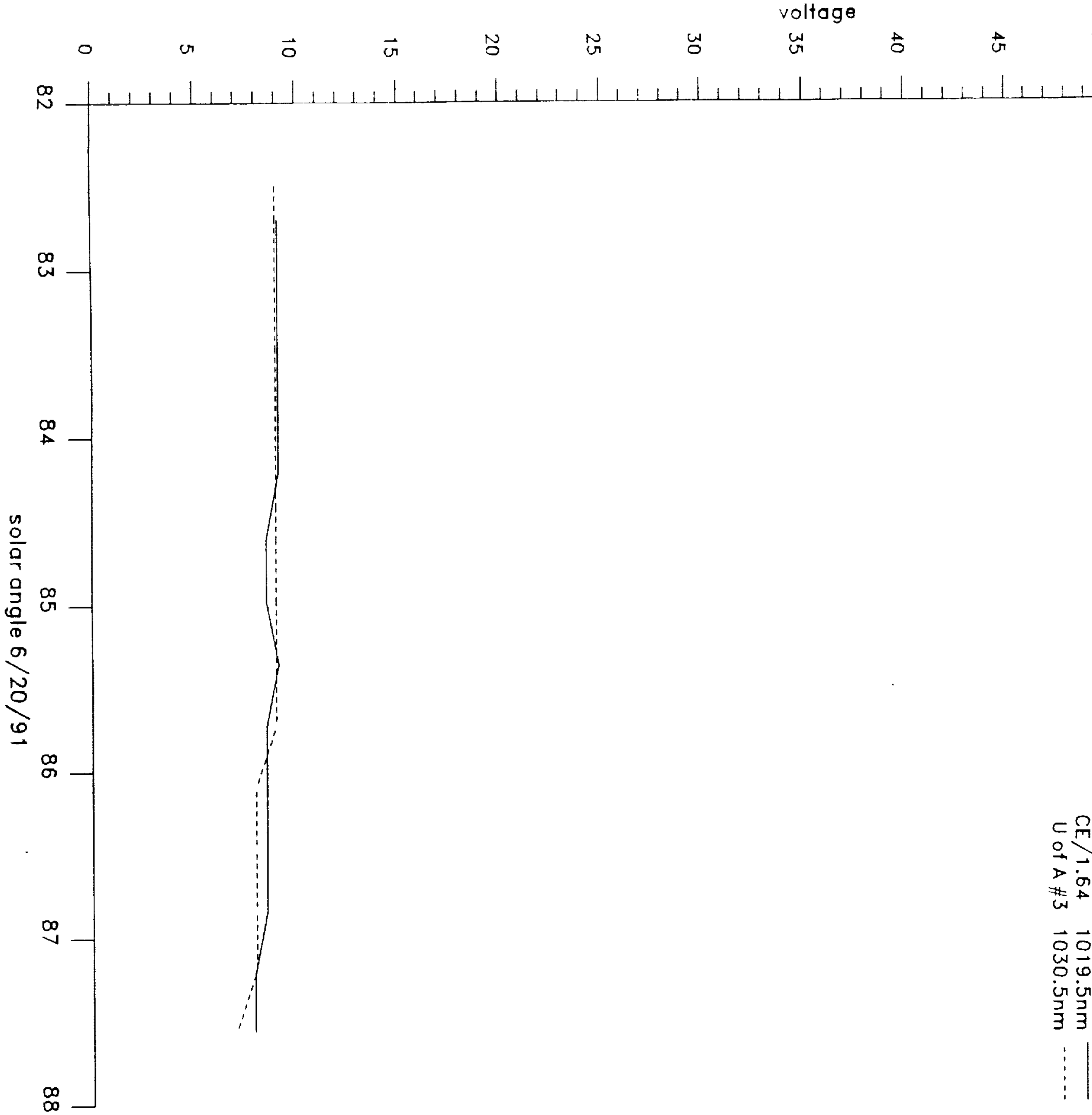
voltage
0
5
10
15
20
25
30
35
40
45
50
82
83
84
85
86
87
88
solar angle 6/20/91
CE/1.64 1019.5nm
U of A #3 1030.5nm

Figure 13

Figure 14

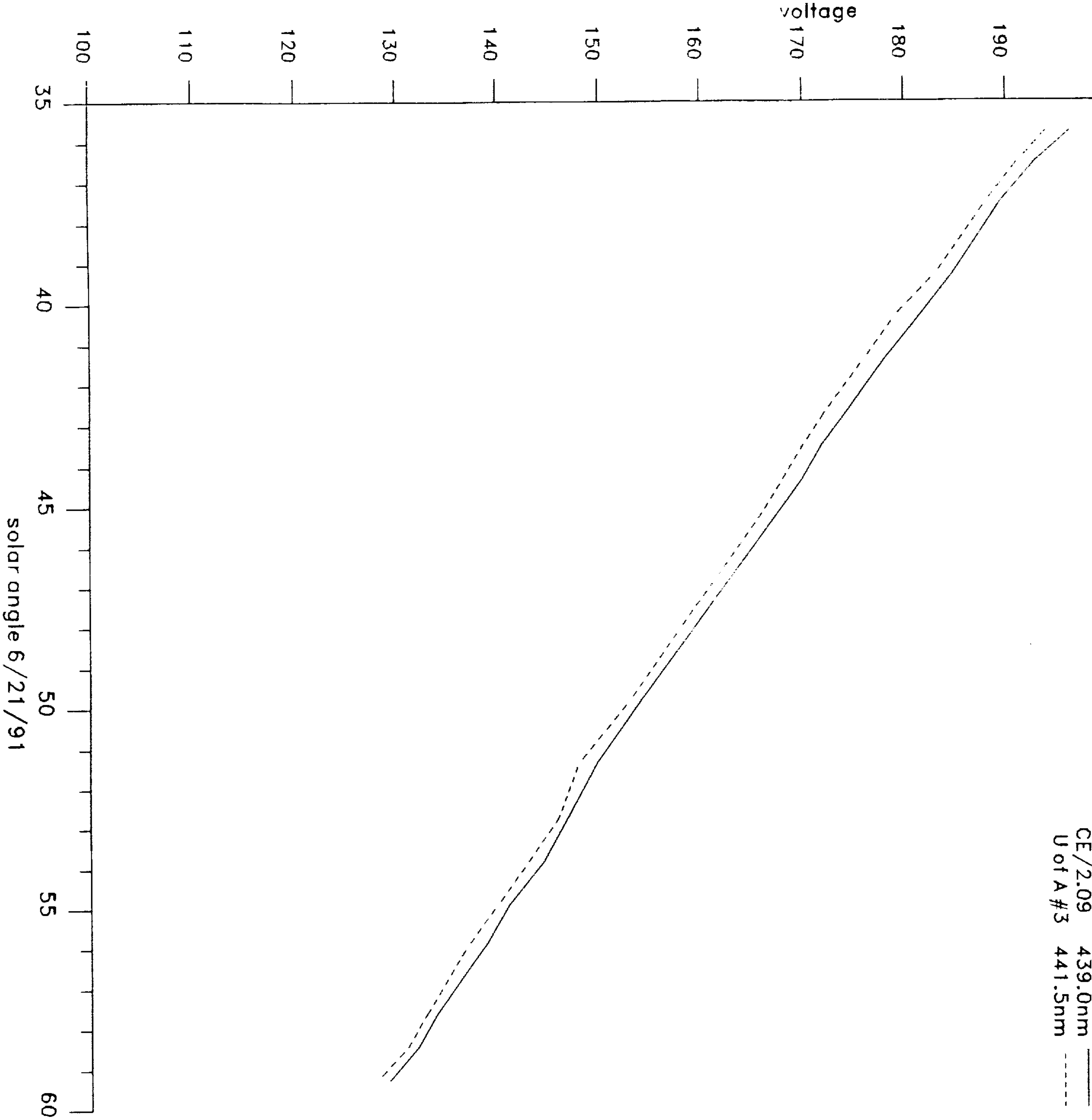
voltage
100
110
120
130
140
150
160
170
180
190
200
35
40
45
50
55
60
solar angle 6/21/91
CE/2.09 439.0nm
U of A #3 441.5nm

Figure 15

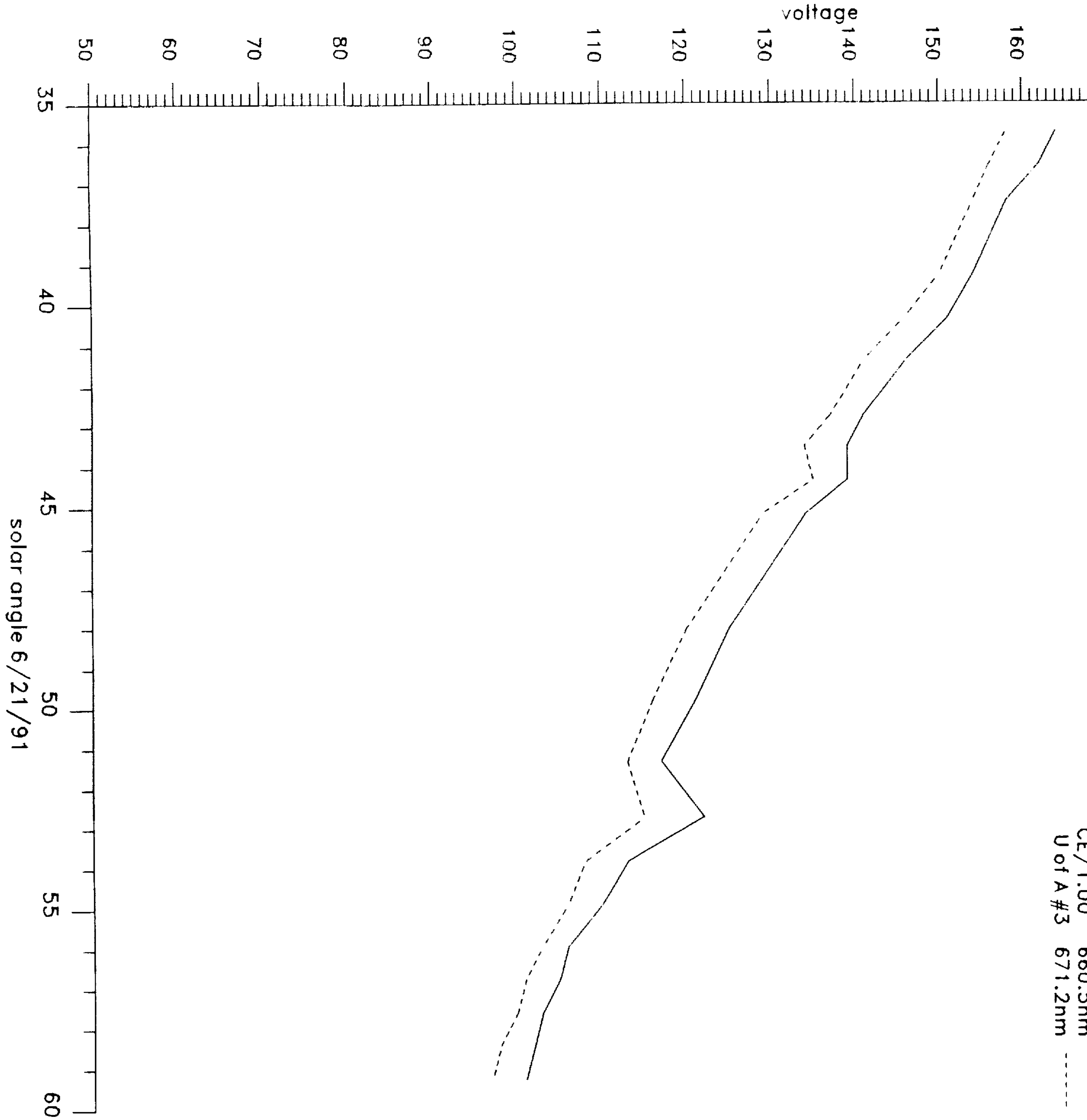
voltage
50
60
70
80
90
100
110
120
130
140
150
160
170
35
40
45
50
55
60
solar angle 6/21/91
CE/1.00 660.5nm
U of A #3 671.2nm

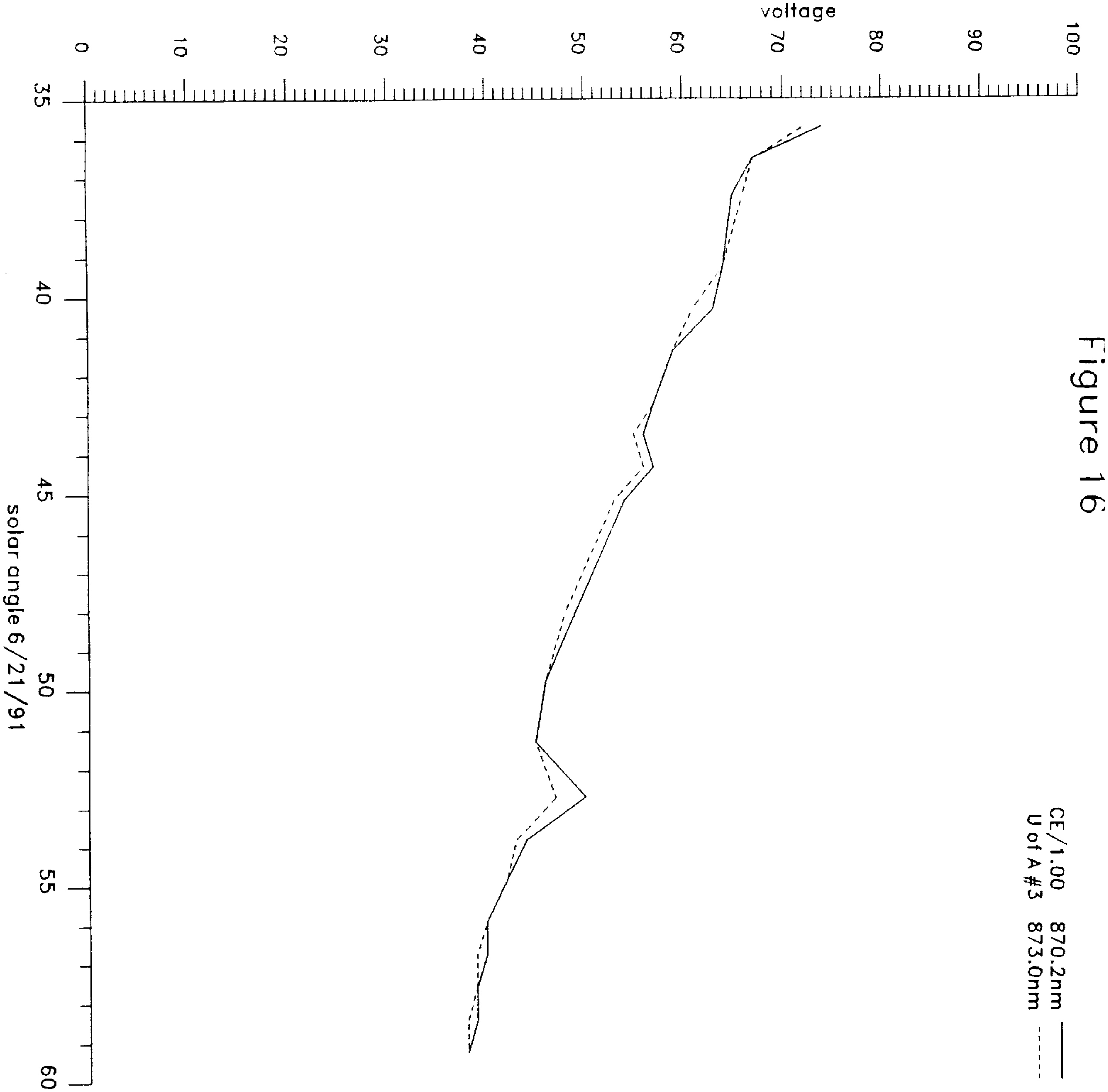
Figure 16
voltage
0
10
20
30
40
50
60
70
80
90
100
35
40
45
50
55
60
solar angle 6/21/91
CE/1.00 870.2nm
U of A #3 873.0nm

Figure 17

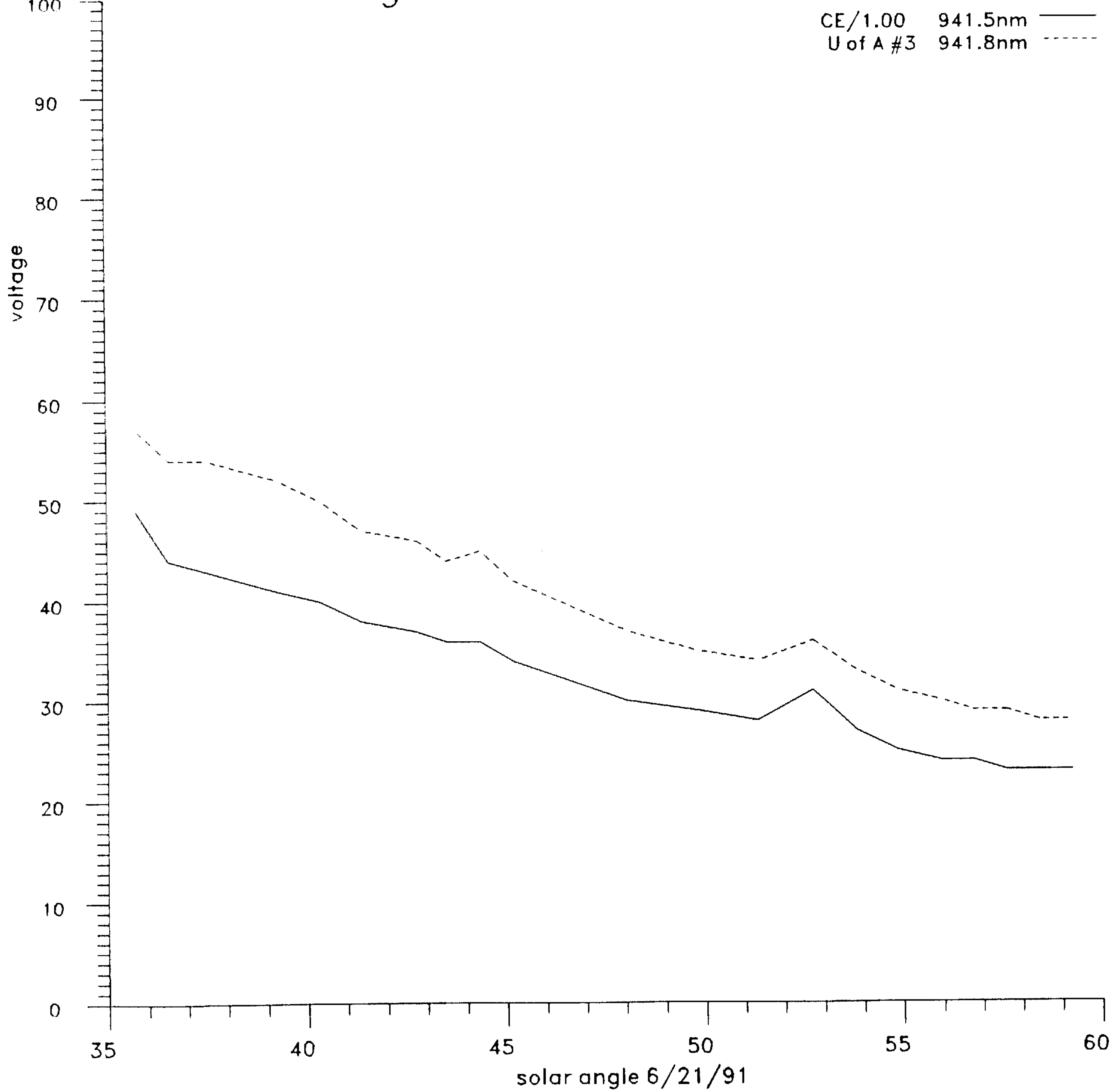

CE/1.00 941.5nm
U of A #3 941.8nm
voltage
0
10
20
30
40
50
60
70
80
90
100
35
40
45
50
55
60
solar angle 6/21/91

Figure 18

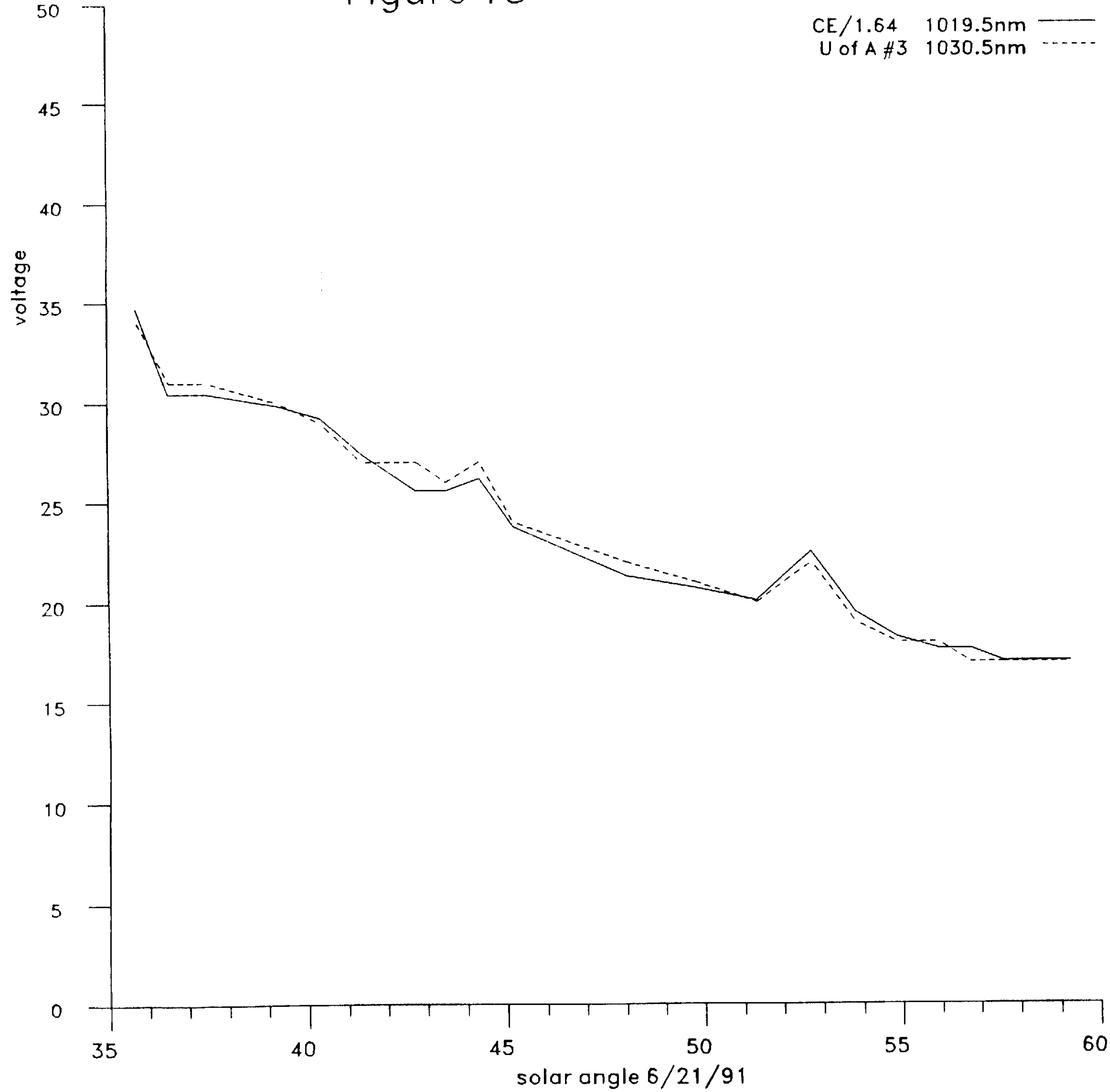
CE/1.64 1019.5nm
U of A #3 1030.5nm
voltage
0
5
10
15
20
25
30
35
40
45
50
35
40
45
50
55
60
solar angle 6/21/91

Figure 19

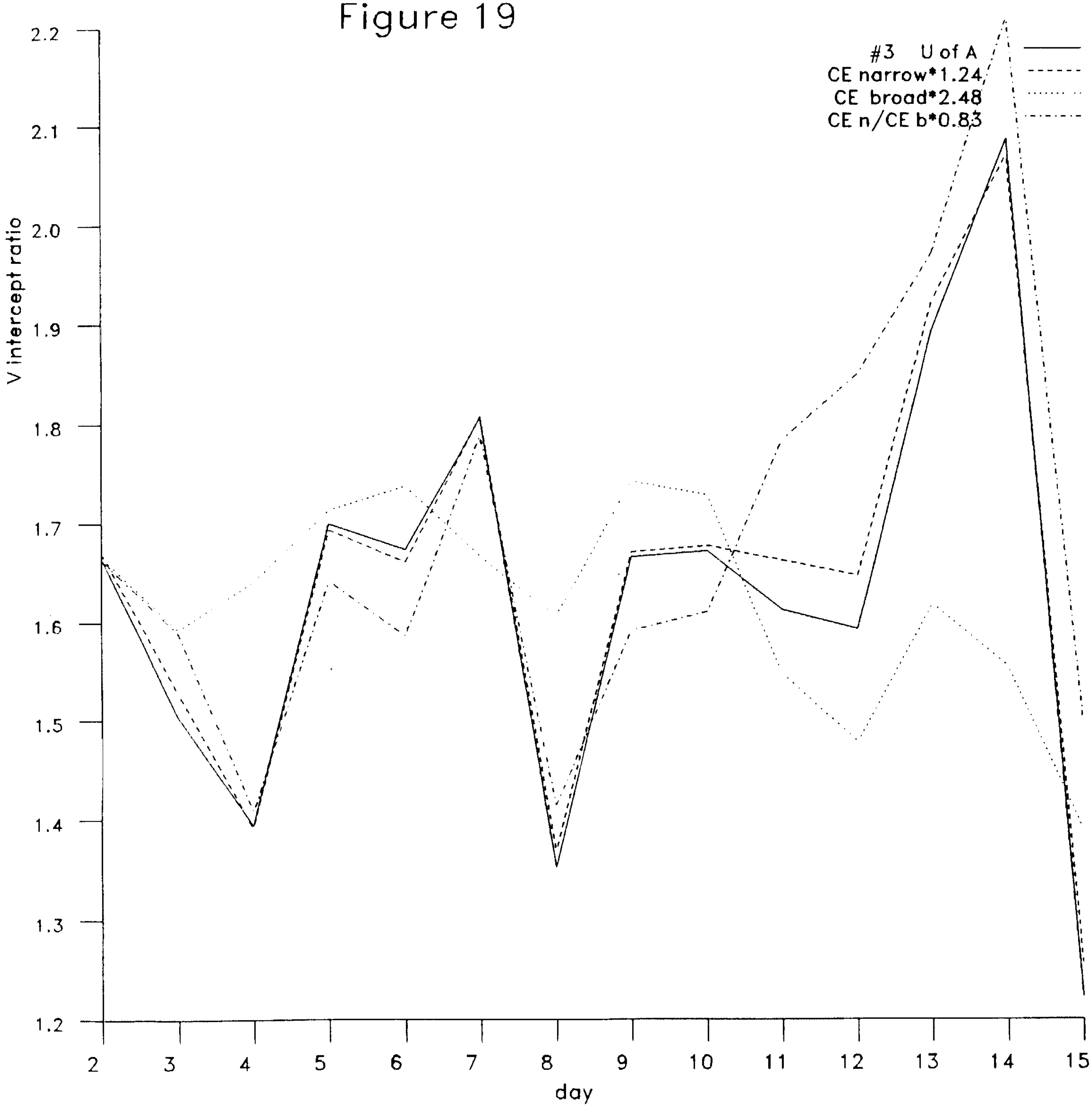

#3 U of A
CE narrow*1.24
CE broad*2.48
CE n/CE b*0.83
V intercept ratio
2.2
2.1
2.0
1.9
1.8
1.7
1.6
1.5
1.4
1.3
1.2
2
3
4
5
6
7
8
9
10
11
12
13
14
15
day

Figure 20 #3 6/21/91

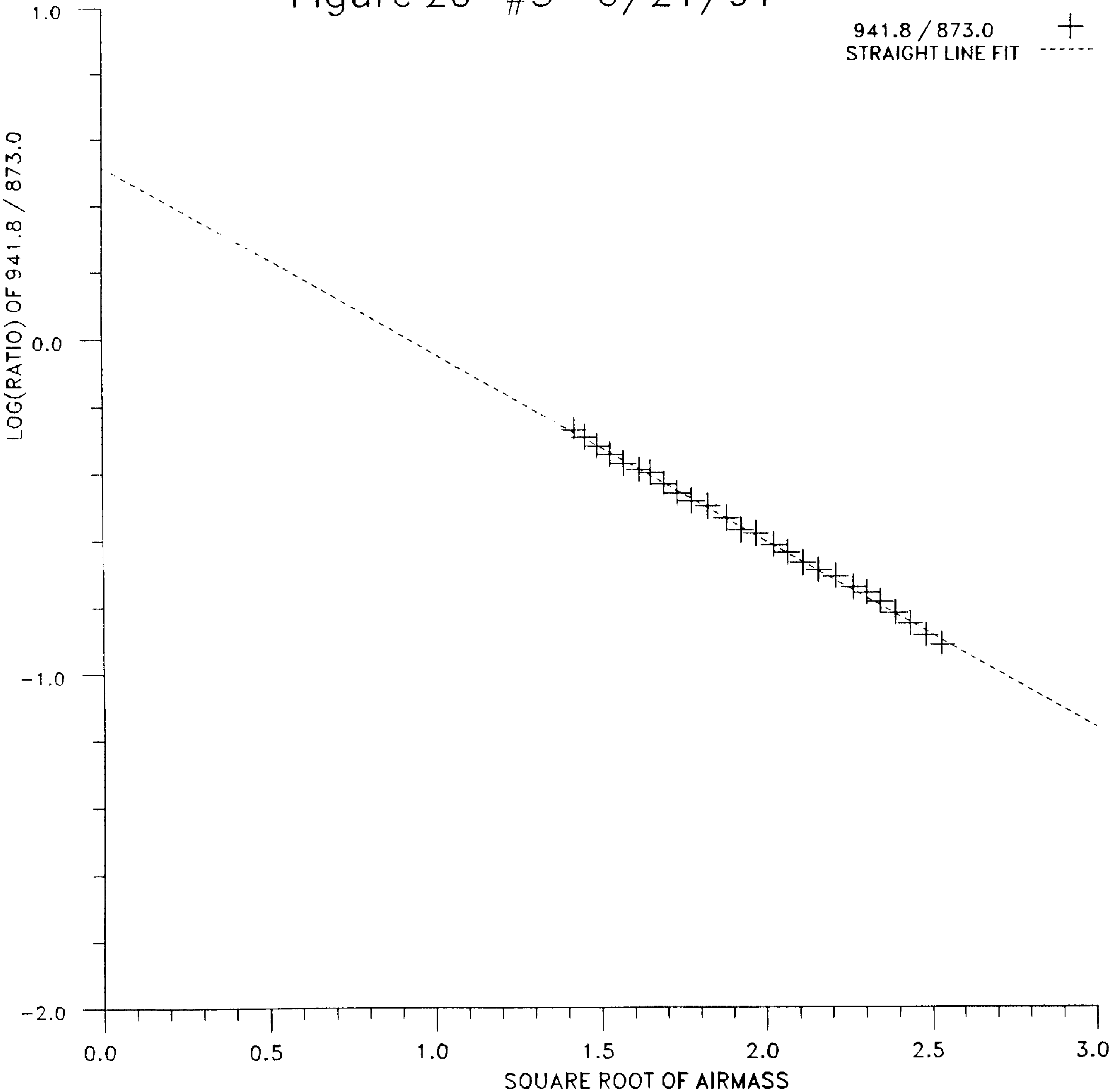

Figure 21 CE 6/21/91

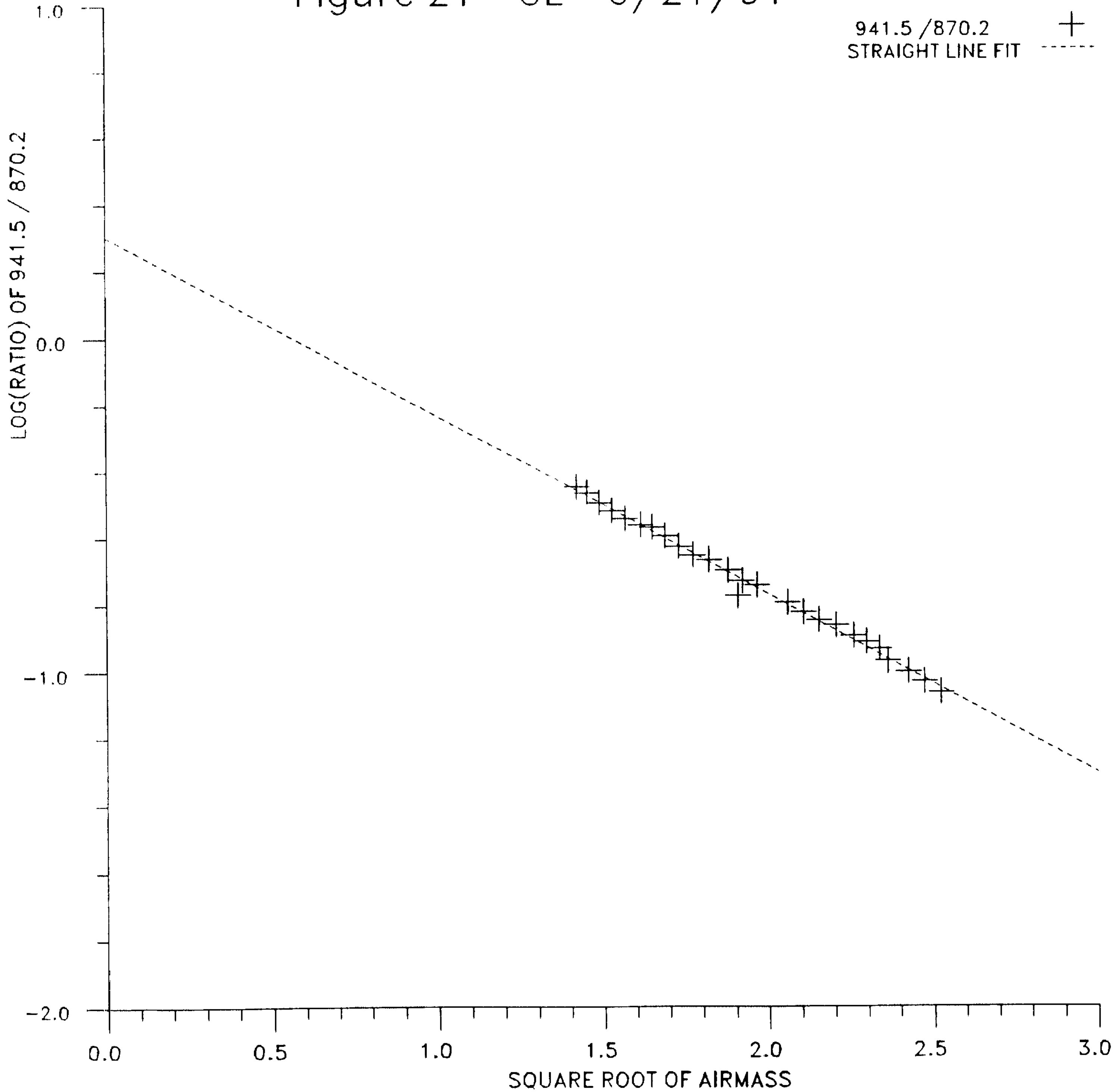

Figure 22 CE 6/21/91

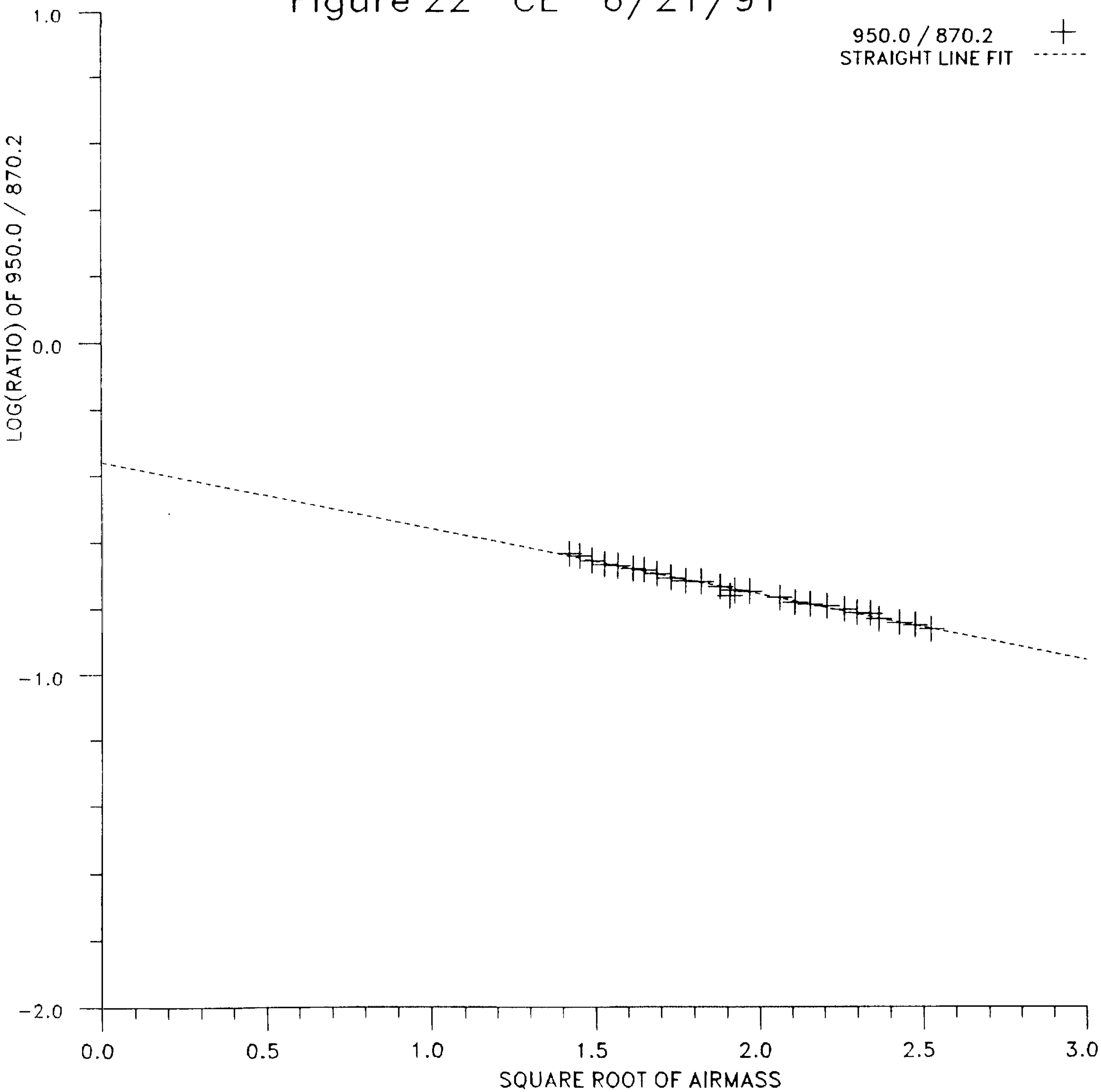

Figure 23 CE 6/21/91